CellPress

Developmental Cell
Matters Arising

Variations in the Efficiency of Lineage Marking and Ablation Confound Distinctions between Myogenic Cell Populations

Glenda Comai,[1,2] Ramkumar Sambasivan,[1,2,3] Swetha Gopalakrishnan,[1] and Shahragim Tajbakhsh[1,*]
[1]Stem Cells and Development, Department of Developmental & Stem Cell Biology, URA CNRS 2578, Institut Pasteur, 25 rue du Dr. Roux, 75015 Paris, France
[2]Co-first author
[3]Present address: Institute for Stem Cell Biology and Regenerative Medicine, GKVK, Bellary Road, Bangalore 560065, India
*Correspondence: shahragim.tajbakhsh@pasteur.fr
http://dx.doi.org/10.1016/j.devcel.2014.11.005

SUMMARY

The myogenic regulatory genes *Myf5*, *Mrf4*, *Myod*, and *Myogenin* likely arose by gene duplications during evolution, presumably to address the more demanding requirements of the vertebrate body plan. Two cell lineages were proposed to be regulated independently by *Myf5* and *Myod* to safeguard against tissue failure. Here we report severe muscle loss following ablation of *Myf5*-expressing cells. Using both lineage-specific and ubiquitous reporter alleles, we show that the remaining muscles in *Myf5*^{Cre}-*DTA* embryos arise mainly from Myf5^{+} escaper cells. Elimination of *Myf5*^{Cre}-*DTA* cells on a *Myod* null background did not result in the total absence of skeletal muscles, as would be expected if a *Myod*$^{+}$/*Myf5*-independent cell population played a major role in this scenario. Therefore, these observations are incompatible with a previously proposed functional two-lineage model. These findings will have an impact on the interpretation of phenotypes obtained using similar strategies in other tissues.

INTRODUCTION

Gene duplications of critical regulatory genes during evolution likely arose to assure the establishment and diversification of tissues as well as survival of the organism in detrimental conditions. Studies in skeletal myogenesis have provided insights into this design where the three cell fate determinants *Myf5*, *Myod*, and *Mrf4* can each autonomously govern myogenic cell identity. Genetic studies in mice where all three genes are compromised in function showed that myoblasts and differentiated cells fail to develop (Kassar-Duchossoy et al., 2004; Rudnicki et al., 1992). Mice mutant for the fourth member of this bHLH family, *Myogenin*, exhibit major differentiation deficits (Tajbakhsh and Buckingham, 2000). The requirement for several cell fate regulators is intriguing, and can be explained in part by their distinct temporal and spatial patterns of activation during myogenic lineage progression (Cossu et al., 1996; Goldhamer et al., 1995; Ott et al., 1991; Sassoon et al., 1989; Tajbakhsh and Buckingham, 2000; Tajbakhsh et al., 1997). For example, during development, *Myf5* expression is highest in the embryonic phase, and it is downregulated during differentiation, whereas *Myod* is expressed in both embryonic and fetal myoblasts and myofibers (Murphy and Kardon, 2011; Tajbakhsh and Buckingham, 2000). In addition, while loss of function of the major myogenic determinants *Myf5* or *Myod* results in skeletal myogenesis in virtually all anatomical locations (Braun et al., 1992; Kablar et al., 1997; Rudnicki et al., 1992; Tajbakhsh et al., 1997), fetal myogenesis fails in *Myf5:Myod* double mutants (Kassar-Duchossoy et al., 2004), demonstrating that these factors can functionally compensate for each other to a large extent.

An unresolved question for many tissues, including skeletal muscle, is whether different fate determinants act within a single, or in distinct cell lineages (Figure 1A). For example, *Neurogenin1* and *Neurogenin2*, bHLH genes that act in the nervous system, were reported to govern distinct sensory cell populations in the chick and mouse (Frank and Sanes, 1991; Ma et al., 1999). Similarly, studies in skeletal myogenesis lead to the proposal that independent progenitor cell lineages functionally incorporate either of the two major regulators, *Myf5* or *Myod,* thereby providing a failsafe mechanism during tissuegenesis (Figure 1A). Specifically, ablation of *Myf5*-expressing cells in an in vitro ES cell differentiation model (Braun and Arnold, 1996), and genetic ablation studies in mice using a conditionally activated diphtheria toxin gene (Gensch et al., 2008; Haldar et al., 2008) were found to be compatible with myogenesis. A pool of Myod^{+} progenitors that did not express *Myf5* by lineage tracing criteria was proposed to compensate for this loss in cranial and somitic mesoderm-derived muscles. These observations could therefore explain in part the requirement for several cell fate determinants and suggest that during evolution, duplications in myogenic regulators (Atchley et al., 1994; Zhao et al., 2014) might have correlated with a duplication of the respective progenitor cell populations.

A two-lineage model is difficult to reconcile with a recent report showing that DTA-mediated ablation of *Myod*-expressing cells results in complete loss of muscle at all anatomical locations (Wood et al., 2013). However, because this result does not formally exclude the possibility of a *Myod*$^{+}$/*Myf5*-independent lineage, resolving these progenitor cell relationships is

critical to understand the dynamics of myogenic cell populations during muscle ontology. Furthermore, this information will affect the interpretation of adult muscle stem cell heterogeneity, and phenotypes of mutants that affect this cell population (Günther et al., 2013; Kuang et al., 2007; von Maltzahn et al., 2013).

Although both somitic and cranial mesoderm-derived muscles have a critical requirement for the three myogenic determination genes, the use of distinct upstream gene regulatory networks in founder stem cells (*Pax3* in trunk and limbs; *Tbx1* and *Pitx2* in cranial mesoderm; Harel et al., 2009; Kelly, 2013; Sambasivan et al., 2009, 2011) raises the possibility that local progenitor cell lineages might also be diverse. Given our previous genetic studies defining distinct gene regulatory networks in cranial- and somite-derived muscles (Sambasivan et al., 2009), we originally performed $Myf5^{Cre}$-driven cell ablation to examine cranial muscle progenitor fates. Unexpectedly, we found severe loss of muscle not only in the head, but also in major muscle groups throughout the organism, implying that if a $Myod^{+}$/*Myf5*-independent population was present, it did not functionally compensate as reported previously (Gensch et al., 2008; Haldar et al., 2008). By tracing *Myf5* progenitors following cell ablation with a number of sensitive reporters, we demonstrate that 100% elimination of *Myf5*-expressing cells cannot be achieved, and instead we propose that $Myf5^{+}$ escaper cells masquerade as an independent $Myod^{+}$ population. Together with the data obtained in a *Myod* null background, we propose that if a $Myod^{+}$/*Myf5*-independent population exists, it is not functionally robust, and thus, not compatible with a two lineage model.

RESULTS

Severe Loss of Muscle in $Myf5^{Cre}$-*DTA* Mice

Previous studies used two different $Myf5^{Cre}$ alleles (Haldar et al., 2007; Tallquist et al., 2000) and two $R26^{DTA}$ mice (one with an attenuated DTA; Brockschnieder et al., 2004; Wu et al., 2006) to ablate *Myf5*-expressing cells (Gensch et al., 2008; Haldar et al., 2008). Skeletal muscles were reported to be initially lacking in the embryo, but this phenotype was rescued and muscles were virtually normal in the fetus. Because the focus of those studies was largely trunk and limb muscles with limited attention to cranial muscles, we assessed the progenitor cell relationships in the head in more detail, where distinct gene regulatory networks initiate myogenesis. We used the same $Myf5^{Cre}$ alleles ($Myf5^{CreCAP}$ and $Myf5^{CreSOR}$; Haldar et al., 2007; Tallquist et al., 2000) crossed with $R26^{DTA}$ mice in which cell death was reported to occur in less than 24 hr after recombination (Ivanova et al., 2005); referred to here as: $Myf5^{Cre}$-*DTA*. Interestingly, the masseter and temporalis, which are two of the major muscle groups in the head, were entirely lacking or severely reduced in size (Figure 1B; Figure S1A available online; and data not shown). Extraocular and other cranial muscle phenotypes also ranged from total absence to severe muscle loss depending on the $Myf5^{Cre}$ line used (Figure 1C; Figure S1B, see below). Approximately 80% of the $Myf5^{CreCAP/+}$:$R26^{DTA/+}$ fetuses examined (n = 6, embryonic day 14.5 [E14.5]; n = 13, E18.5) displayed a cleft of the secondary palate (Figure 1B; Figures S1A and S1C), which is consistent with a requirement for mechanical stimuli from the adjacent masseter for proper palatogenesis (Rot and Kablar, 2013; Rot-Nikcevic et al., 2006). $Pax7^{+}$ and $Myod^{+}$ cells were absent from regions of muscle ablation, with rare cells sparsely located among rudimentary myofibers (Figure 1B inset; Figure S1C; and data not shown). Therefore, progenitor cells were also lacking in regions where muscle masses were lost in $Myf5^{Cre}$-*DTA* embryos.

Unexpectedly, analysis of limb and trunk muscles at E18.5 also revealed severe muscle loss (Figure 1D, and Figure S1D). In general, forelimbs were more severely affected than hindlimbs (not shown). Accordingly, 100% of the $Myf5^{CreCAP/+}$:$R26^{DTA/+}$ fetuses examined showed relaxed forepaws, reduced dorsiflexion, and lack of deltoid tuberosity (Figure 1E, n = 55; and Figure S1E, n = 7), which are phenotypes resulting from loss of muscle masses (Blitz et al., 2009; Nowlan et al., 2010; Rot-Nikcevic et al., 2006). We performed immunostainings for skeletal muscle-specific myosin heavy chain (MyHC) on transverse forelimb cryosections of E18.5 control and $Myf5^{CreCAP}$-*DTA* fetuses at different levels along the proximo-distal axis (Figure 1D). Quantifications of the MyHC positive area per cross-sectional area showed a significant reduction in the total muscle area in $Myf5^{CreCAP}$-*DTA* fetuses (Figure 1F), in agreement with the observations in E14.5 embryos (Figures S1F and S1G). As with ablated cranial muscles, no $Pax7^{+}$ cells were present at sites of muscle loss (data not shown). Therefore, cranial- and somite-derived muscles were ablated using both *Cre* alleles, indicating that myogenesis was not completely rescued by a second *Myf5*-independent progenitor population as previously reported. We note that although all muscle groups were not missing in every fetus examined, collation of data across large sample sizes (n > 24 embryos cryosectioned, n = 55 animals total) showed that several muscle groups were susceptible to partial or full loss, independent of body region (Figure 1G and data not shown). As a striking example, the esophagus, which contains a layer of circular and longitudinal skeletal muscles, totally lacked skeletal muscles in all $Myf5^{CreCAP}$-*DTA* fetuses, with no rescue at any stage examined (n = 7; Figure 1H). These observations raised questions as to why all muscles groups were not ablated with the genetic combinations used. We therefore performed combinations of expression analysis and independent genetic validation experiments to address this point and reconcile our results with those of previous reports where muscles were reported to be virtually normal in $Myf5^{Cre}$-*DTA* fetuses (Gensch et al., 2008; Haldar et al., 2008).

Incomplete Ablation of *Myf5*-Expressing Cells in $Myf5^{Cre}$-*DTA* Embryos

To examine the efficiency of DTA-mediated ablation of *Myf5*-expressing cells and the efficacy of the *Cre*-expressing *Myf5* alleles, we generated $Myf5^{nlacZ/Cre}$:$R26^{DTA}$ compound heterozygous embryos. $Myf5^{nlacZ}$ embryos provide the advantage of using the more sensitive β-gal activity to report *Myf5* expression independently of Cre activity. In addition, persistence of β-gal activity can be used as a lineage tracer at later stages to mark cells that had historically experienced *Myf5* expression in the progenitor state independent of contemporary Myf5 protein expression (Cossu et al., 1996; Tajbakhsh et al., 1996a; Tajbakhsh and Buckingham, 2000). Strikingly, we found significant amounts of X-gal-stained $Myf5^{nlacZ}$-positive cells persisting in virtually all anatomical locations with both *Cre* alleles (Figure 2A). This result was unexpected given that *Myf5* expression is highest between E8.5 and E11.5 (Ott et al., 1991) and efficient cell

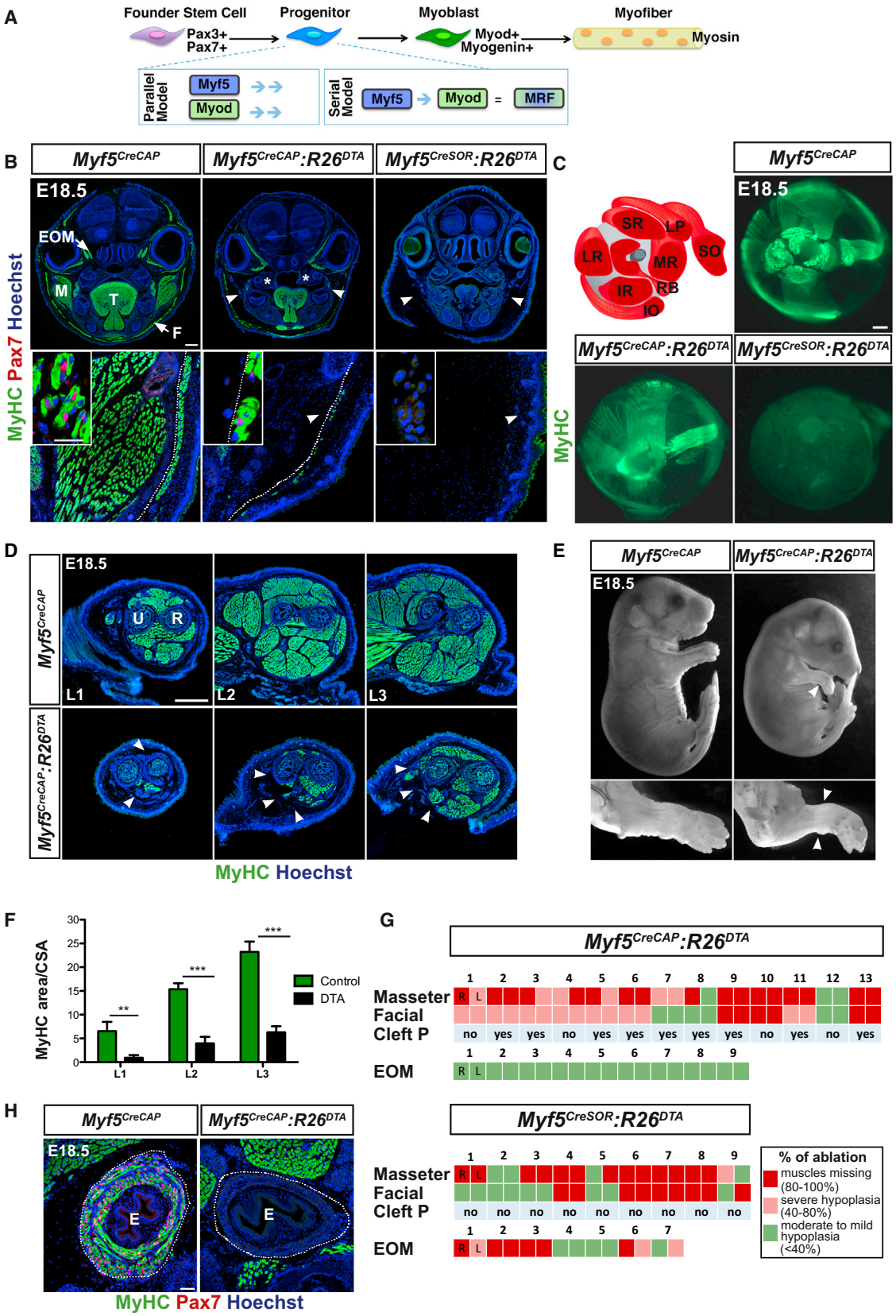

(legend on next page)

death should have occurred by E12.5 if *Cre* had been expressed faithfully in *Myf5*-positive cells. Furthermore, extensive amounts of $Myf5^{nlacZ}$-positive cells were detected in E14.5 ablated embryos, well after reduction in the expression level of the *Myf5* gene, and after ample time for the ablation to take place (Figure S2A).

We then used our recently reported sensitive, lineage-specific, *Pax7*-driven reporter allele as a control for monitoring recombination efficiency ($Pax7^{nGFP\text{-}stop\text{-}nlacZ}$ hereafter called $Pax7^{GPL}$; Sambasivan et al., 2013). Given that *Pax7* is expressed in skeletal muscle stem/progenitor cells, accessibility of this locus to *Cre*-mediated recombination allows higher sensitivity for tracking cells within the muscle lineage (Relaix and Zammit, 2012; Sambasivan et al., 2013). We first tested if the $Pax7^{GPL}$ reporter is an appropriate reporter for these studies. We compared the recombination efficiency of $Pax7^{GPL}$ and $R26^{mTmG}$ reporters in cells enzymatically isolated from limbs and trunks of $Myf5^{CreCAP/+}$::$Pax7^{GPL/+}$::$R26^{mTmG/+}$ E13.5 and E18.5 embryos (Figures S2B and S2C). Immunostaining with anti-Pax7, anti-GFP, and anti-β-gal antibodies showed that more than 95% of trunk $Pax7^+$ cells recombined the $Pax7^{GPL}$ reporter by E13.5 (Figure S2B). Recombination of the ubiquitous $R26^{mTmG}$ reporter followed the same trend but appeared somewhat less efficient. Similar results were obtained when scoring β-gal$^+$ and/or GFP$^+$ cells over the total number of trunk Myod$^+$ cells, on limb cell preparations (Figure S2C) and on E12.5 and E14.5 cryosections from $Myf5^{CreCAP/+}$:$Pax7^{GPL/+}$ embryos (Figures S2D and S2E; data not shown). Together, these observations show not only that the $Pax7^{GPL}$ reporter could be used as a faithful reporter for our cell ablation studies, but also that virtually all Pax7$^+$ and Myod$^+$ progenitor cells have been primed by *Myf5* by the end of the embryonic phase. This is in agreement with previous reports, demonstrating that the majority of satellite cell founders are primed by *Mrf4* (Sambasivan et al., 2013) and *Myod* (Kanisicak et al., 2009) prenatally. Given this condition, we expect that the $Myf5^{Cre}$-*DTA* ablation should report in a similar manner, i.e., that the entire population should be ablated.

Analysis of $Myf5^{Cre/+}$::$Pax7^{GPL/+}$::$R26^{DTA/+}$ fetuses using both *Cre* drivers ($Myf5^{CreCAP}$ and $Myf5^{CreSOR}$) at E14.5 and E17.5 showed that in cranial and somitic muscles, massive amounts of β-gal-expressing cells remained (Figure 2B; Figures S2F–S2H). Therefore, $Myf5^{Cre}$ mediated recombination of the $Pax7^{GPL}$ locus occurred, but these β-gal$^+$ cells were not eliminated by the DTA. In addition, these experiments using the $Myf5^{nlacZ}$ and $Pax7^{GPL}$ reporters showed severe loss of muscle following ablation of *Myf5*-expressing cells, similar to the data in Figure 1 in the absence of any reporter. One issue using this ablation strategy concerns the timing of *Myf5*-expression and the time required for DTA to kill these cells. We note that with both of these reporters, X-gal$^+$ nuclei were observed within surviving myofibers in all body locations (Figure S2F and data not shown). Because *Myf5* is not expressed in myofibers (Gayraud-Morel et al., 2012; Ott et al., 1991; Tajbakhsh and Buckingham, 2000), and in accordance with the persistence of these X-gal-stained muscles in the fetus, we expect that the muscles that were derived from *Myf5*-expressing cells would no longer be ablated.

Despite extensive studies with both *Myf5* and *Pax7*, haploinsufficiency has not been reported for these genes during prenatal myogenesis (Relaix and Zammit, 2012; Shi and Garry, 2006; Tajbakhsh and Buckingham, 2000; Yin et al., 2013). Nevertheless, to circumvent an unanticipated haploinsufficiency issue entirely, in particular in the context of cell ablation, we performed complementary experiments using whole-mount MyHC stainings in the absence of reporters (Figure 2C). These stainings gave the same results as quantifications on tissue sections (Figure 1D), namely severe loss or reduction in muscles in $Myf5^{Cre}$-*DTA* fetuses. Higher variation between individuals and higher amounts of muscle remained with $Myf5^{CreSOR}$, which is likely due to higher numbers of $Myf5^+$ escapers (see Figures S2H and S2I). Importantly, the β-gal$^+$ cells that remained following ablation using the $Myf5^{nlacZ}$ and $Pax7^{GPL}$ reporters did not stain for cleaved-caspase3 at E12.5, E13.5, and E14.5, indicating that these cells were not dying at these relatively late

Figure 1. Severe Loss of Muscle in $Myf5^{Cre}$-*DTA* Fetuses

(A) Schemes illustrating lineage progression during myogenesis. The bottom line depicts the two principal myogenic determination genes *Myf5* and *Myod* acting either in a single (serial model) or in distinct (parallel model) progenitor cell populations.

(B) Masseter muscle was ablated using two $Myf5^{Cre}$ alleles (CAP, n = 13; SOR, n = 9; arrowheads). Anti-MyHC (green) and anti-Pax7 (red) immunostainings of E18.5 coronal head cryosections. Higher magnification images of masseter regions (bottom, insets) indicate absence of Pax7$^+$ muscle stem/progenitor cells in areas lacking muscle. Asterisks highlight the presence of cleft palate. Dotted lines delimit masseter from facial muscles. M, masseter; T, tongue; EOM, extraocular muscle; F, facial muscle.

(C) Whole-mount MyHC immunostaining of E18.5 eyeballs as in scheme. Extraocular muscles are generally reduced in size ($Myf5^{CreCAP/+}$:$R26^{DTA/+}$; n = 9, 18 eyeballs assessed) or can be completely missing ($Myf5^{CreSOR/+}$:$R26^{DTA/+}$; n = 7, 14 eyeballs assessed). SO, superior oblique; LP, levator palpebrae; SR, superior rectus; LR, lateral rectus; MR, medial rectus; IR, inferior rectus; IO, inferior oblique; RB, retractor bulbi.

(D) Anti-MyHC staining of E18.5 fetal limbs showing severe reduction in size and missing muscle masses (arrowheads) in $Myf5^{CreCAP/+}$:$R26^{DTA/+}$ fetuses (n = 4). Sections at different levels of the proximo-distal axis of the forelimb zeugopod are depicted as L1, L2, and L3 (see Figure S1E). R, radius, U, ulna (bones frequently trap antibody).

(E) Macroscopic views of E18.5 $Myf5^{CreCAP/+}$:$R26^{DTA/+}$ and control fetuses. Note that mutant fetus is smaller with an abnormal posture. Lower images highlight relaxed forepads and reduced dorsiflexion (arrowheads) observed in 100% of $Myf5^{CreCAP/+}$:$R26^{DTA/+}$ fetuses (n = 55).

(F) Quantification of the total myogenic zone (MyHC$^+$ staining/cross-sectional area, mean ± SEM) at three different levels (L1, L2, L3) in the forelimbs of E18.5 controls ($Myf5^{CreCAP/+}$ and $R26^{DTA/+}$; n = 3) and $Myf5^{CreCAP/+}$:$R26^{DTA/+}$ (n = 4) fetuses. Right and left limbs were scored for each animal. Note severe deficit in forelimb muscle mass in $Myf5^{Cre}$-*DTA* fetuses.

(G) Table summarizing muscle phenotypes with two $Myf5^{Cre}$ alleles in $Myf5^{Cre}$-*DTA* E18.5 embryos; n values are shown on top. L, left; R, right muscles. Extraocular muscles belong to different embryo sets because whole-mount immunostainings were used for comparison.

(H) Anti-MyHC (green) and anti-Pax7 (red) immunostaining on transverse trunk cryosections reveal complete ablation of the skeletal muscle of the esophagus in $Myf5^{CreCAP/+}$:$R26^{DTA/+}$ fetuses (n = 7) at E18.5. The esophagus (E) is delineated with a dotted line. Adjacent neck muscles are not ablated in $Myf5^{Cre}$-*DTA* fetuses. Scale bars in (B) represent 500 μm, high power 25 μm; (C), 200 μm; (D), 500 μm; and (H), 50 μm. See also Figure S1.

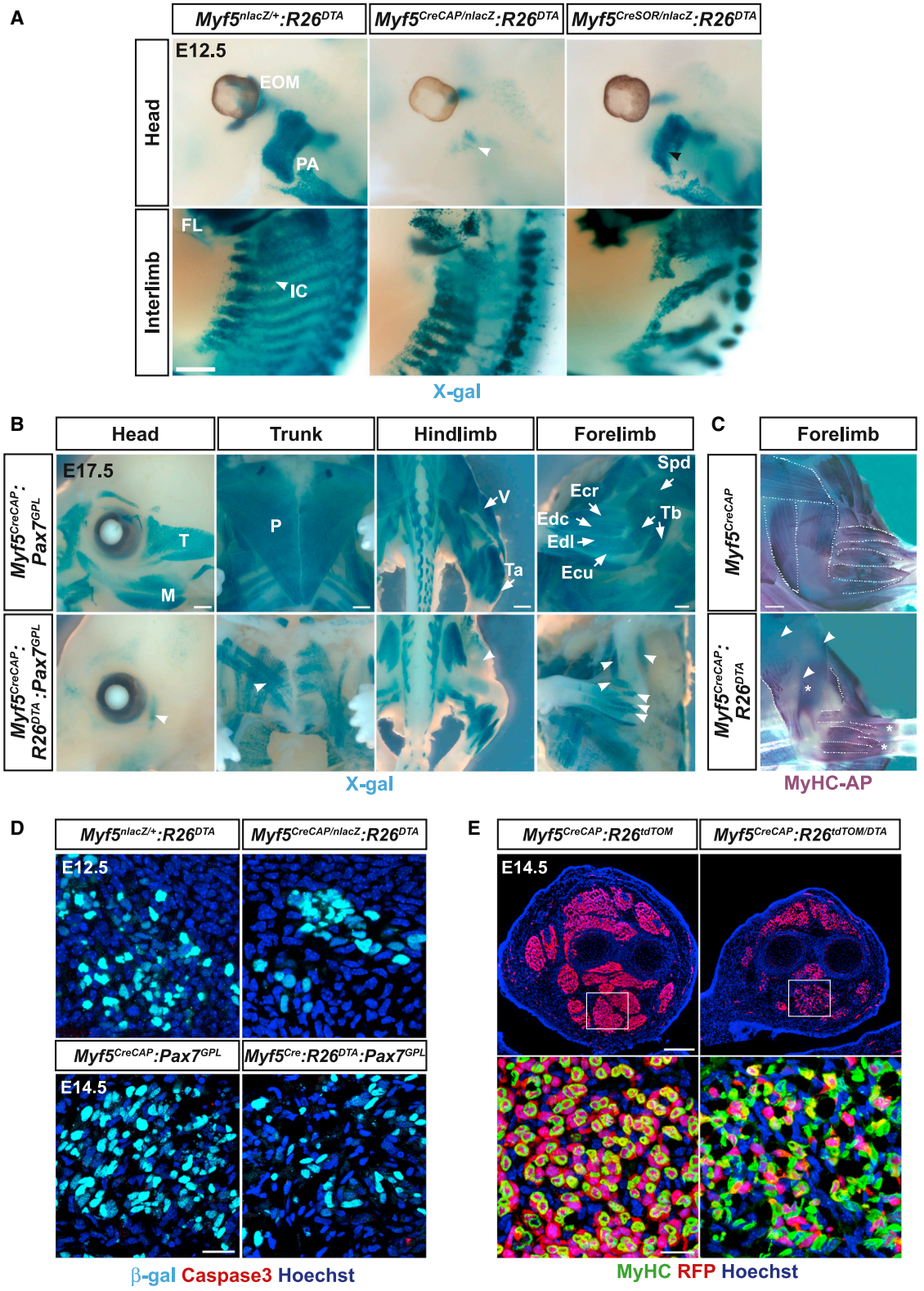

Figure 2. Lineage-Specific and Ubiquitous Reporters Reveal Failure to Ablate *Myf5*-Expressing Cells in *Myf5*^{Cre}-*DTA* Embryos

(A) X-gal stained E12.5 *Myf5*$^{nlacZ/+}$:*R26*$^{DTA/+}$ and *Myf5*$^{nlacZ/Cre}$:*R26*$^{DTA/+}$ embryos. β-gal^{+} cells persist in *Myf5*$^{nlacZ/Cre}$:*R26*$^{DTA/+}$ embryos, indicating failure to ablate all *Myf5*-expressing cells. Upper images show patterning of cranial muscle anlagen (Extraocular [EOM] and pharyngeal arch [PA] muscles). Note that PA muscle anlagen is severely ablated in *Myf5*^{CreCAP} embryos (white arrowhead, middle) (n = 4) whereas ablation is less severe in *Myf5*^{CreSOR} embryos (n = 3) (black

(legend continued on next page)

stages (Figure 2D; Figure S2J—control for staining; and data not shown).

To confirm these findings, we combined *Myf5*^{CreCAP}:*R26*^{DTA} with another commonly used lineage reporter that is expressed ubiquitously. *Ai9* is a universal *Rosa26*-derived reporter line in which the strong CAG promoter drives conditional expression of *tdTomato* (Madisen et al., 2010). In agreement with our results obtained using both *Myf5*^{nlacZ} and *Pax7*^{GPL} reporters, remaining nonablated tdTomato$^+$ cells were found in E14.5 *Myf5*$^{CreCAP/+}$::*R26*$^{DTA/+}$::*R26*$^{tdTOM/+}$ fetuses in MyHC$^+$ regions of the limb (Figure 2E) and trunk (data not shown).

Taken together, these results demonstrate the existence of nonparallel recombination between two *Rosa*-based reporters (*R26*^{DTA} and *R26*^{tdTOM}) as well as *Rosa*-based and lineage-specific reporters (*R26*^{DTA} and *Pax7*^{GPL}) within genetically identical cells. Therefore, the data clearly point to the presence of a significant population of *Myf5*-derived nonablated cells contributing to the muscles remaining in *Myf5*^{Cre}-*DTA* embryos and fetuses.

Extensive Contribution of *Myf5*-Derived Myogenic Cells to Myogenesis in *Myf5*^{Cre}-*DTA* Embryos

Having established that *Myf5*-derived nonablated cells remain in the *Myf5*^{Cre}-*DTA* embryos, we next assessed the contribution of the presumed Myod$^+$/*Myf5*-independent cells. For a two-lineage model to be valid as reported, all remaining *Myod*-expressing cells in *Myf5*^{Cre}-*DTA* embryos should be reporter-negative (not *Myf5*-derived). Quantifications on *Myf5*$^{Cre/+}$::*Pax7*$^{GPL/+}$::*R26*$^{DTA/+}$ embryos showed β-gal$^-$ Myod$^+$ cells interspersed with β-gal$^+$ Myod$^+$ cells (Figure 3A). This result suggests that a presumed Myod$^+$/*Myf5*-independent cell population (based on reporter-negativity) and nonkilled Myod$^+$/*Myf5*-derived cells contribute to muscle rescue in *Myf5*^{Cre}-*DTA* embryos. To assess the relative contribution of each subpopulation, we examined the proliferative status of β-gal and/or Myod-expressing cells with EdU labeling (4–5 hr pulse) in the trunk muscles of *Myf5*$^{CreCAP/+}$::*Pax7*$^{GPL/+}$::*R26*$^{DTA/+}$ embryos at different developmental stages (Figures 3A and 3B).

In *Myf5*^{Cre}-*DTA* embryos at E12.5, 29% of the total Myod$^+$ cell population was positive for the reporter (β-gal$^+$, nonablated, *Myf5*-derived), and 70% of these cells were found to be proliferating (EdU$^+$). The β-gal$^-$ Myod$^+$ cells, which also likely includes Pax3$^+$ Pax7$^-$ progenitor-derived cells and potentially, the presumed *Myf5*-independent pool, represented a major fraction (71%) of the total Myod$^+$ cells, yet only 30% of these cells were proliferating (Figure 3B; p values on Figure S3A). We note here that a major fraction of β-gal$^-$ Myod$^+$ cells were also Myogenin$^+$ (83% at E12.5, n = 3); therefore, differentiated and exited the cell cycle (data not shown). By E14.5, the situation evolved significantly. β-gal$^+$ Myod$^+$ cells (*Myf5*-derived nonkilled) expanded substantially and contributed to 50% of the total Myod$^+$ population in *Myf5*^{Cre}-*DTA* embryos, with half of these cells still in proliferation (Figure 3B). Therefore, these data suggest that by E14.5, two apparent subpopulations (*Myf5*-derived and *Myf5*-independent) contribute to similar extents to muscle rescue in *Myf5*^{Cre}-*DTA* embryos. We note that the presumed *Myf5*-independent population was designated as such based solely on reporter negativity.

Similar results were obtained with the ubiquitous *R26*^{tdTomato} line. In this case, more than 95% of the Myod$^+$ cells in the control were reporter$^+$ at E14.5 (Figures S3B and S3C). In *Myf5*^{Cre}-*DTA* embryos, the nonablated reporter$^+$ cells (55%) contributed to a similar extent as the reporter$^-$ cells (45%) to muscle rescue in the *Myf5*^{Cre}-*DTA* embryos.

Finally, we evaluated the efficiency of rescue by examining *Pax7* expression. In E12.5 control embryos, more than 96% of the Pax7$^+$ cells were *Pax7*^{GPL} reporter$^+$, and 68% of these cells were proliferating. In *Myf5*^{Cre}-*DTA* embryos, up to 66% of the total Pax7$^+$ cells were reporter$^+$ (β-gal$^+$, nonablated, *Myf5*-derived), where 77% of these cells were proliferating. This indicates that a major proportion of the proliferating Pax7$^+$ population present in *Myf5*^{Cre}-*DTA* embryos were derived from nonablated *Myf5*-expressing cells (Figures S3D and S3E). Similar results were obtained at E14.5 (data not shown).

Taken together, these results indicate that *Myf5*-derived nonablated myogenic cells (Pax7$^+$ or Myod$^+$) contribute as much or more than the presumed *Myf5*-independent (reporter$^-$) cells to muscle rescue in *Myf5*^{Cre}-*DTA* embryos. As far as the contribution of reporter-negative cells is concerned, additional validations of the genetically modified mice are necessary to ascertain their true origins. To address this point directly, we examined the fidelity of *Cre* expression from the *Myf5* locus as well as the efficacy of *DTA*-mediated cell ablation.

Nonconcordance between Modified *Cre* Allele and Endogenous *Myf5* Expression

Although we noted a severe loss of muscle in *Myf5*^{Cre}-*DTA* embryos, muscles that remained were largely reporter$^+$

arrowhead, right). Lower images show variation in the pattern and severity of somitic muscle ablation between *Myf5*^{CreCAP} and *Myf5*^{CreSOR} mutants (intercostal, IC; forelimb, FL). *Myf5*$^{nlacZ/CreSOR}$:*R26*$^{DTA/+}$ genetic combination is null for *Myf5*, whereas this is not the case for *Myf5*$^{nlacZ/CreCAP}$:*R26*$^{DTA/+}$ (*IRES-Cre*).

(B) Whole-mount macroscopic analysis of representative muscle groups in *Myf5*$^{CreCAP/+}$:*Pax7*$^{GPL/+}$ and *Myf5*$^{CreCAP/+}$::*R26*$^{DTA/+}$::*Pax7*$^{GPL/+}$ E17.5 fetuses (n = 3) stained with X-gal. Note that in the latter, major cranial and somitic muscle groups are lacking or severely reduced (arrowheads). M, masseter; T, temporoparietal; P, pectoralis major; Ta, tibialis anterior; V, vastus; SpD, spinodeltoid; Tb, triceps brachii; Ecu, extensor carpi ulnaris; Ecr, extensor carpi radialis; Edc, extensor digitorum communis; Edl, extensor digitorum longus.

(C) Lateral views of forelimbs from *Myf5*$^{CreCAP/+}$ and *Myf5*$^{CreCAP/+}$:*R26*$^{DTA/+}$ E17.5 fetuses (n = 5) stained by whole-mount immunohistochemistry for myosin heavy chain (MyHC-AP, alkaline phosphatase). Dotted lines delineate individual forelimb muscles, which are severely reduced in the mutant, and arrowheads point to missing muscles. Asterisks indicate endogenous alkaline phosphatase activity in the bones, which are not covered by muscle in the mutant.

(D) Immunostainings on trunk sections of E12.5 *Myf5*$^{nlacZ/+}$:*R26*$^{DTA/+}$ and *Myf5*$^{nlacZ/CreCAP}$:*R26*$^{DTA/+}$ embryos (n = 3) and E14.5 *Myf5*$^{CreCAP/+}$:*Pax7*$^{GPL/+}$ and *Myf5*$^{CreCAP/+}$::*R26*$^{DTA/+}$::*Pax7*$^{GPL/+}$ embryos (n = 2) with anti-β-gal (cyan) and anticleaved caspase3 (red) antibodies. Note the persistence of β-gal$^+$ cells that are not dying in *Myf5*^{Cre}-*DTA* embryos.

(E) Immunostainings of E14.5 forelimb sections of *Myf5*$^{CreCAP/+}$:*R26*$^{tdTOM/+}$ and *Myf5*$^{CreCAP/+}$:*R26*$^{tdTOM/DTA}$ embryos (n = 2) with anti-MyHC (green) and anti-RFP (red) antibodies. Note that *Myf5*-derived RFP$^+$ cells remain in *Myf5*^{Cre}-*DTA* embryos.

Scale bars in (A) represent 200 μm; (B) and (C), 100 μm; (D), 25 μm; and (E), 200 μm, high power 20 μm. See also Figure S2.

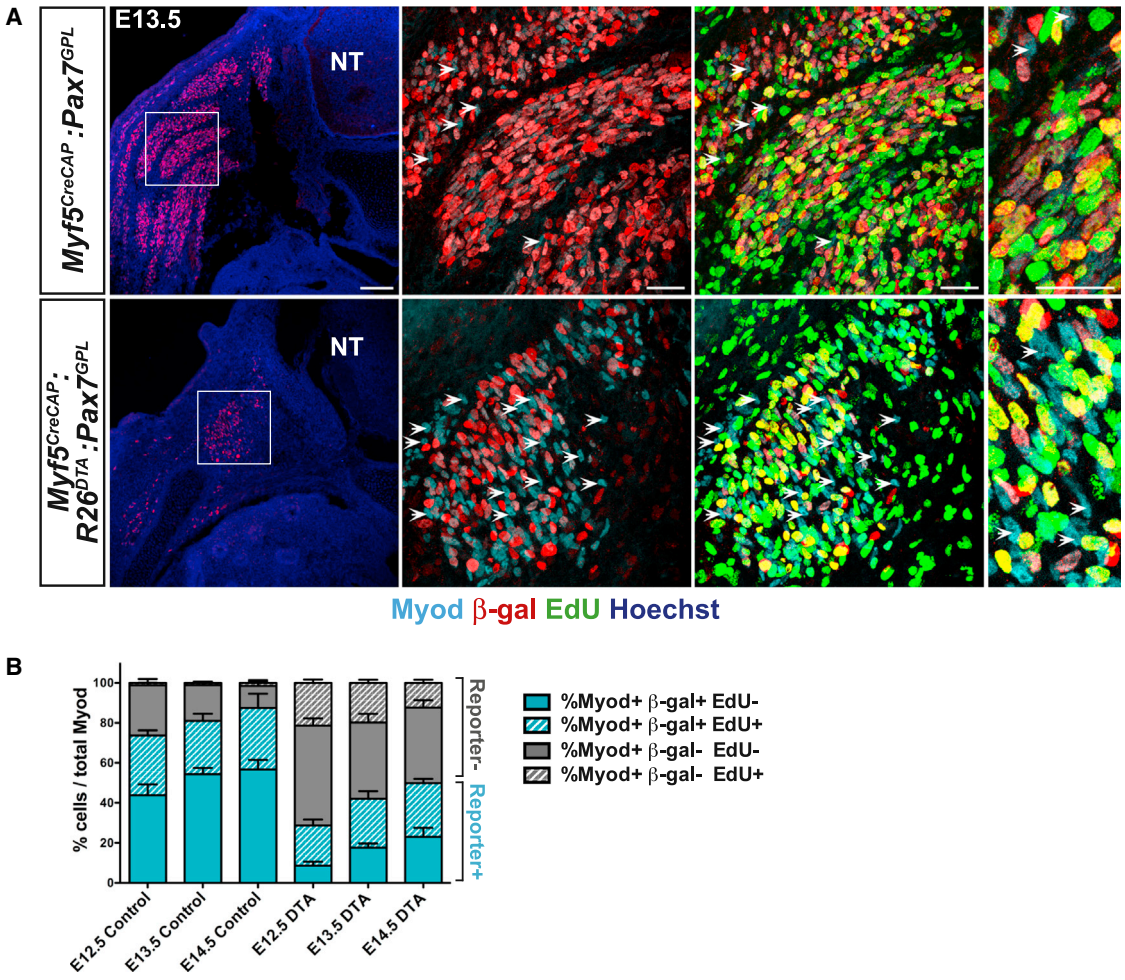

Figure 3. Contribution of *Myf5*-Derived Nonkilled Myogenic Cells and Putative *Myf5*-Independent Cells to Muscle Rescue in $Myf5^{Cre}$-*DTA* Embryos

(A and B) Quantitation of the percentage of proliferating cells derived from Myf5-expressing and Myf5-independent cell populations in $Myf5^{CreCAP/+}$:$Pax7^{GPL/+}$ and $Myf5^{CreCAP/+}$::$R26^{DTA/+}$::$Pax7^{GPL/+}$ embryos at E12.5 (n = 3), E13.5 (n = 3), and E14.5 (n = 2). Between 650 and 1,400 cells were counted per genotype and per condition.

(A) Representative picture of the immunostainings performed with anti-β-gal (red), anti-Myod (cyan) and EdU (green) staining. Note reduction in muscle masses in the trunk of $Myf5^{Cre}$-*DTA* embryos (left: NT, neural tube). White arrows point to $Myod^+$ β-gal^- cells that are not proliferating.

(B) Histograms of control and $Myf5^{Cre}$-*DTA* embryos show statistically significant differences in the percentage of $Myod^+$ βgal^+ EdU^-, $Myod^+$ βgal^- EdU^-, and $Myod^+$ βgal^- EdU^+ populations at the respective time points (mean ± SEM, p values on Figure S3A). The percentage of $Myod^+$ βgal^+ EdU^+ cells (e.g., proliferating cells derived from *Myf5*-lineage derived) is not statistically different between control and $Myf5^{Cre}$-*DTA* embryos.

Scale bars in (A) represent low power 100 μm, high powers 25 μm. See also Figure S3.

(*Myf5*-derived), indicating that all of the *Myf5*-expressing cells were not eliminated. One possibility is that the $R26^{DTA}$ allele was either not recombined or expression of *DTA* from the *R26* locus was not sufficient to ablate all of the *Myf5*-expressing cells. When we investigated the recombination efficiency of the $Myf5^{Cre}$ alleles by examining $R26R^{lacZ}$ reporter activity, significant variations in the extent of *lacZ* expression were observed between the different *Cre* alleles, as well as between embryos of the same litter (Figure S4A, data not shown). Different *Rosa*-based reporters are known to have variable susceptibility for recombination (Liu et al., 2013). Nevertheless, an intrinsic recombination deficiency is not likely to be the sole explanation for the incomplete ablation in our $Myf5^{Cre}$-*DTA* embryos because the same conditional *R26* promoter-driven DTA lines were effective in killing all muscles in $Myog^{Cre}$:$R26^{DTA}$ (Gensch et al., 2008; $R26^{lacZ\text{-}DTA}$), $Myod^{Cre}$:$R26^{DTA}$ (Wood et al., 2013; $R26^{eGFP\text{-}DTA}$), and $ACTA1^{Cre}$:$R26^{DTA}$ (data not shown; $R26^{eGFP\text{-}DTA}$) genetic combinations where the *Cre* driver was used with genes that have persistent expression in the lineage.

Another possibility is that *Cre* levels from the *Myf5* locus are insufficient to allow complete elimination of *Myf5*-expressing cells. If that were the case, one would hypothesize that cells expressing high levels of *Cre* are killed efficiently, thereby resulting in severe loss of muscle; cells expressing lower levels of *Cre* might not recombine the $R26^{DTA}$ allele and therefore not be killed. To investigate this possibility, we examined *Myf5* and

Cre expression with in situ hybridization (ISH). Using a 5′UTR probe for *Myf5* transcripts and in accordance with the persistence of *Myf5*-reporter$^+$ cells noted above, significant levels of endogenous *Myf5* transcripts were observed in somites and limbs of E10.5 *Myf5^{Cre}-DTA* embryos (Figure 4A). Importantly, *Cre* expression was severely reduced and constituted only a subset of *Myf5* expression pattern even in control nonablated embryos. Expression of *Myod* was also reduced in *Myf5^{Cre}-DTA* embryos, indicating that DTA ablation was functional and a high proportion of *Myod*-expressing cells were *Myf5*-derived (Figure 4A). Because DTA is an inhibitor of translation, we performed ISH at later stages to allow enough time for complete ablation of *Myf5*$^+$ cells. At E11.5, *Myf5*-expressing cells remained using two different *R26^{DTA}* ablator mouse alleles (Brockschnieder et al., 2004; Ivanova et al., 2005), one of which (*Myf5^{CreSOR}:R26$^{lacZ\text{-}DTA}$*) is the same genetic combination reported previously (Gensch et al., 2008; Figures S4B and S4C). At E13.5, the *Myod* ISH pattern highlighted the loss of muscle masses in the limbs (Figures 4B and S4D) as observed above with whole-mount immunostaining, and with the *Cre*-dependent reporters. Strikingly, *Myf5*-expressing cells could be still detected in the limbs of E13.5 *Myf5^{CreCAP}-DTA* embryos, but *Cre* expression was lacking (Figures 4B and S4D). In addition, allele-specific RT-qPCR of *Myf5^{Cre}* heterozygous embryos showed a 2- to 5-fold reduction in *Cre* expression from the *Myf5$^{IRES\text{-}CreCAP/+}$* allele compared to the unmodified *Myf5* allele (data not shown). Therefore, the genetically altered bicistronic *(IRES)-Cre* allele showed reduced expression compared to the endogenous locus.

Finally, we examined the expression of Cre and Myf5 proteins with immunohistochemistry (Figure 4C). Myf5 and Cre were coexpressed to a certain extent in trunk muscle masses of E11.5 and E12.5 control embryos. At E13.5, Cre protein was not detected in wild-type embryos in the trunk, consistent with the downregulation of the *Myf5* locus at this stage; however, cells expressing low levels of Cre were detected in the limbs, which is consistent with the normal developmental timing for Myf5 expression in this location (data not shown). In agreement with the data presented above, we found that Myf5$^+$ cells persisted in the trunks of E11.5, E12.5, and E13.5 *Myf5$^{CreCAP/+}$:R26$^{DTA/+}$* embryos; however, these cells did not express detectable levels of Cre protein. This observation suggests that high Cre-expressing cells were ablated, whereas the remaining *Myf5*-expressing cells were not. Given this finding that Cre expression is severely downregulated in *Myf5^{Cre}-DTA* embryos, one can no longer assume with confidence that the reporter$^-$ cells observed above constitute a bona fide Myf5-independent lineage.

Skeletal Muscles Persist in *Myf5^{Cre}-DTA* Mice Lacking *Myod*

To assess directly whether the β-gal$^-$ cells in the genetic lineage tracing studies above are indeed a *Myf5*-independent/*Myod*-derived lineage, we decided to perform the ablation of *Myf5*-expressing cells in a *Myod* null background. If two cell lineages are indeed present during the establishment of skeletal muscles, a total absence of myogenesis should be expected in *Myf5$^{CreCAP/+}$::R26$^{DTA/+}$::Myod$^{-/-}$* embryos. Strikingly, we could not detect a statistically significant difference in the amount of skeletal muscles remaining in the limbs of E18.5 *Myf5$^{CreCAP/+}$:R26$^{DTA/+}$* compared to *Myf5$^{CreCAP/+}$::R26$^{DTA/+}$::Myod$^{-/-}$* fetuses (Figures 5A and 5B; n = 4). In addition, *Myf5$^{CreCAP/+}$::R26$^{DTA/+}$::Myod$^{-/-}$* embryos had relaxed forepads as observed in *Myf5$^{CreCAP/+}$:R26$^{DTA/+}$* embryos (Figure S5A). Pax7$^+$ cells were observed in remaining muscles of *Myf5$^{CreCAP/+}$::R26$^{DTA/+}$*and *Myf5$^{CreCAP/+}$::R26$^{DTA/+}$::Myod$^{-/-}$* fetuses (Figure 5A). Higher numbers of Pax7$^+$ cells were observed among the muscle masses of *Myod$^{-/-}$* fetuses, with or without cell ablation, in agreement with previous analyses of *Myod* null adult mice (Asakura et al., 2007; Macharia et al., 2010; Figure 5A). Extraocular and trunk muscles were also present in E13.5 and E18.5 *Myf5$^{CreCAP/+}$::R26$^{DTA/+}$::Myod$^{-/-}$* embryos, which was comparable to that of *Myf5^{CreCAP}:R26^{DTA}* embryos (Figure S5B and data not shown). These results lead us to conclude that the presumed *Myod*$^+$/*Myf5*-independent (reporter$^-$) population, if real, makes a minor contribution, if any, to rescue of muscles, and that escaper Myf5$^+$ cells are largely responsible for establishing myogenesis in *Myf5^{Cre}-DTA* embryos.

DISCUSSION

How tissues are established from stem and progenitor cell populations and how this ontology contributes to the adult stem cell pool remain a major unresolved question for most tissues. The observation that adult muscle stem cells are heterogeneous (Kuang et al., 2007; Rocheteau et al., 2012; Shinin et al., 2006; Tajbakhsh, 2009) raises the possibility that distinct founder cell populations that persist during development give rise to this diversity. Two models for skeletal myogenesis have been proposed (Figure 1A): (1) a serial lineage model in which a single progenitor pool expresses the Mrfs subsequently within the same lineage, and (2) a parallel lineage model in which these genes would be expressed in distinct lineages. Based on lineage tracing and conditional cell ablation studies in mice, Haldar and colleagues put forth a parallel lineage model where mutually exclusive *Myf5*-derived and *Myod*$^+$/*Myf5*-independent populations exist during skeletal myogenesis. Using the same strategy, a second report arrived to similar conclusions (Gensch et al., 2008). Notably, *Mrf4* expression was reported to be unchanged or even reduced in *Myf5^{Cre}-DTA* early and late stage embryos (Gensch et al., 2008; Haldar et al., 2008), and this was verified in the present study (Figures S5C and S5D), thereby ruling out a compensatory role for this determination gene (Kassar-Duchossoy et al., 2004) in the muscle rescue observed. Therefore, the authors concluded that the *Myf5*-lineage is dispensable for myogenesis as a *Myod*-lineage takes over when the *Myf5*-lineage is eliminated. Importantly, the observation of rescue to virtually normal myogenesis throughout the body prompted the authors to qualify the *Myod*$^+$/*Myf5*-independent lineage as functionally relevant.

For this model to be valid, several criteria should be fulfilled. First, achievement of 100% ablation of the *Myf5* lineage is an absolute requirement for proposing the existence of a second *Myf5*-independent lineage. Therefore, 100% efficiency of both the *Cre* driver and reporter/ablator lines must be assured. Second, the developmental time course of expression of the gene being evaluated should provide sufficient time for the ablation to take place. Thus, even if the window of opportunity of the gene is tight (e.g., gene being rapidly downregulated) there should be no risk of incomplete kill (Figure 5C, see below).

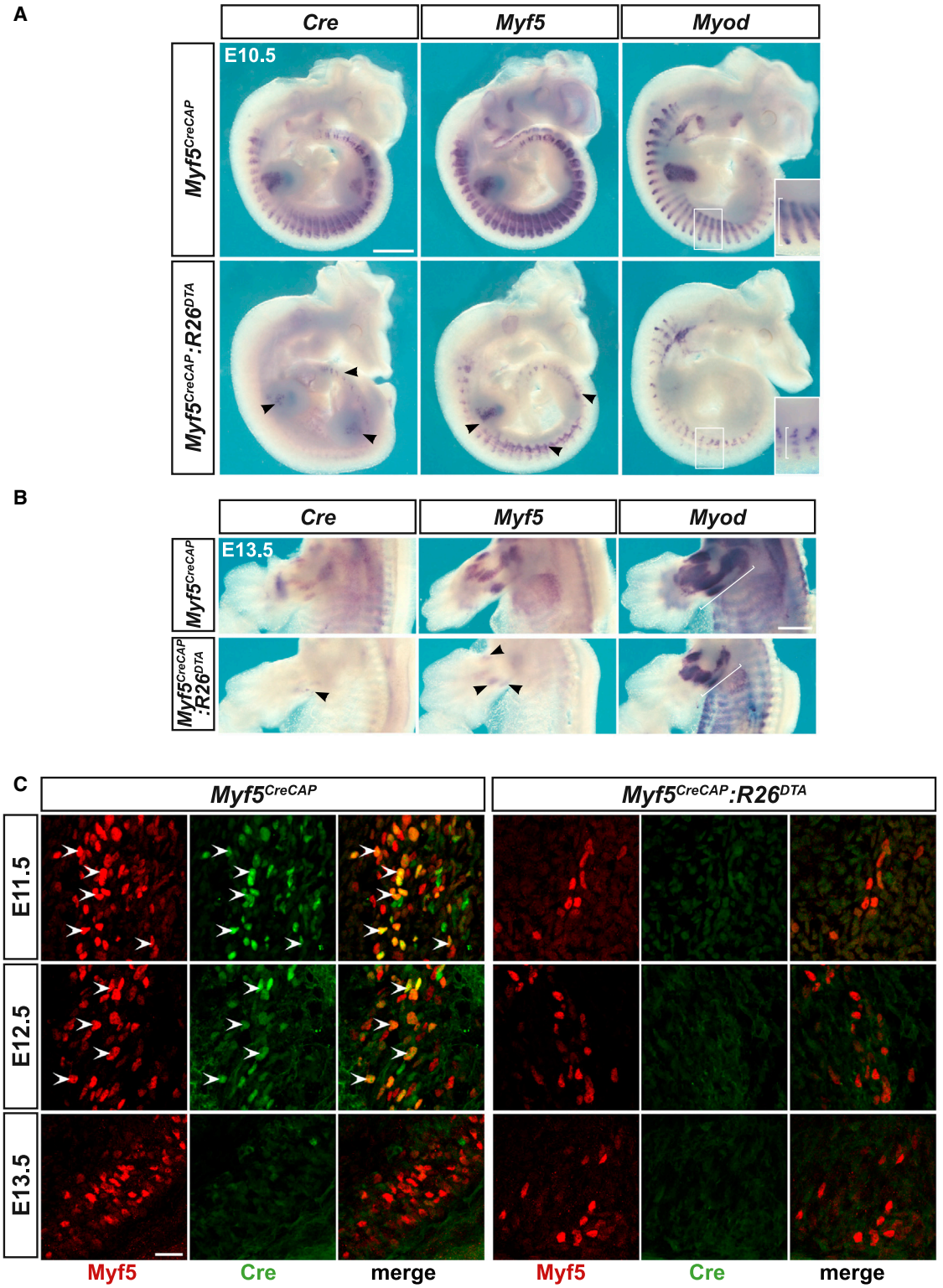

Figure 4. Nonconcordance of *Cre* Expression Compared to Endogenous *Myf5* Expression

(A and B) Assessment of *Cre, Myf5*, and *Myod* transcript levels by whole mount in situ hybridization in E10.5 (A) or E13.5 (B) $Myf5^{CreCAP/+}$ and $Myf5^{CreCAP/+}$:$R26^{DTA/+}$ embryos.

(A) Note that in E10.5 $Myf5^{Cre}$-*DTA* embryos *Cre* transcripts are highly reduced and only present at the level of the forelimbs and tail, whereas *Myf5* transcripts are much more prominent (black arrowheads). *Myod* levels are also lower than the control. The myotome is severely affected (inset).

(legend continued on next page)

Using an extensive array of genetic approaches combined with genetic ablation studies on a large cohort of embryos, we obtained several lines of evidence that fail to support the model of two functional separate myogenic lineages (*Myf5*-derived and *Myod*$^{+}$/*Myf5*-independent) that drive developmental myogenesis independently of one another. First, in contrast with the previous report showing restoration to "virtually normal myogenesis" by early fetal stages following ablation of the *Myf5*-expressing cell population, we observed severe and consistent loss of skeletal muscle at different anatomical locations when using the same genetic approaches. Second, we show that 100% elimination of *Myf5*-expressing cells in *Myf5*^{Cre}*-DTA* embryos is not achieved with any of the reporter mice used (one ubiquitous and two lineage specific; see below). Furthermore, we demonstrate that the partial muscle rescue observed in *Myf5*^{Cre}*-DTA* embryos is contributed largely by *Myf5*-derived, nonablated cells and not exclusively by a presumed *Myod*$^{+}$/*Myf5*-independent (reporter^{-}) population as previously postulated by Haldar and colleagues. In addition, we found that *Cre* expression from *Myf5*^{CreCAP} allele is lost or extremely reduced in *Myf5*^{Cre}*-DTA* embryos at different developmental stages. We propose that in this context, unfaithful *Cre* expression not only leads to incomplete elimination of *Myf5*-expressing cells, but also results in Myf5^{+}/Cre^{-} cells that masquerade as the presumed "*Myod*$^{+}$/*Myf5*-independent (reporter^{-}) lineage." Finally, we challenged the existence of a *Myod*$^{+}$/*Myf5*-independent cell lineage directly. We demonstrated that ablation of Myf5^{+} cells on a *Myod* null background did not eliminate all the skeletal muscles, which would be expected if a *Myod*$^{+}$/*Myf5*-independent lineage was the sole contributor to muscle rescue in *Myf5*^{Cre}*-DTA* embryos. Taken together, these results are incompatible with a second functional *Myod*$^{+}$/*Myf5*-independent lineage as proposed by Haldar and colleagues (and Gensch et al., 2008), and they strongly point to escaper Myf5^{+} cells as the major contributors to myogenesis in *Myf5*-ablated embryos.

Several factors might explain the different conclusions obtained from our studies and those performed previously. A possible key factor is the genetic background used for these types of studies. Extensive literature is available on dramatically different phenotypes obtained for genetically modified mice bred on different genetic backgrounds (http://www.jaxmice.jax.org), although phenotypes are often more severe on purebred backgrounds, which was not the case here.

We believe that the discordance with previous reports can be principally attributed to the inadequacies of genetically modified mice, as we now show using an extensive array of controls. Several studies have demonstrated incomplete recombination with different conditional reporters due to a number of factors such as the chromosomal location of floxed alleles, distance between loxP sites, sequences flanking the loxP sites, stochastic epigenetic mechanisms underlying transgene variegation, and the level of Cre activity per cell (Lewandoski, 2001; Long and Rossi, 2009; Ma et al., 2008; Nagy, 2000; Sambasivan et al., 2013; Vooijs et al., 2001). Therefore, the interpretation of ablation studies solely based on selected reporter alleles is a high-risk task, particularly when the requirement of 100% ablation of a cell population is an obligate prerequisite for support of such a model.

In this respect, several factors can influence the interpretation of the results. First, whereas the previous studies showed loss of *Cre*-dependent reporter expression in *Myf5*^{Cre}*-DTA* embryos (using Z/EG and Z/AP conditional transgenic reporters; Gensch et al., 2008; Haldar et al., 2008), their data did not exclude the existence of Myf5^{+} cells in which both the reporter and *DTA* allele remained unrecombined due to insufficient levels of Cre (see below). In the present study, the introduction of the *Myf5*^{nlacZ} reporter gave us the advantage of using the more sensitive β-gal activity to report *Myf5* expression independently of Cre activity. In addition, we benefited from the persistence of β-gal activity as a lineage tracer at later stages to mark cells that had historically experienced *Myf5* expression in progenitor cells independent of contemporary Myf5 protein expression.

Second, it is now well established that the Z/EG and Z/AP reporters used in the previous studies to score ablation efficiency have the lowest sensitivity to *Cre*-mediated recombination, which is more problematic in cells with low levels of Cre activity (Liu et al., 2013; Ma et al., 2008; data not shown). This is attributed to its high inter-loxP distance (Liu et al., 2013) and makes it unsuitable for tracking cell ablations, especially when it is used to demonstrate the existence of independent cell lineages. Indeed, our comparative analysis demonstrates clearly that Z/AP reporter sensitivity is a major issue (Figure 5D).

In the present study, we used the newer generation *Rosa26*-based *Ai9* line, which is considered as one, if not the most, sensitive *Rosa*-based reporter available (Liu et al., 2013; Madisen et al., 2010), as well as the lineage-specific *Pax7*^{GPL} line as reporters for cell ablation. We showed that while both reporters recombined efficiently, the *R26*^{DTA} fails to do so and therefore only a subpopulation of myogenic cells was efficiently ablated. Moreover, using the *Pax7*^{GPL} reporter, we showed that virtually all Pax7^{+} and Myod^{+} progenitor cells are derived from *Myf5*-expressing cells, and given this condition, we should expect that the *Myf5*^{Cre}*-DTA* ablation reports in a similar manner, i.e., ablates the entire population—which is clearly not the case. These data demonstrate the existence of nonparallel recombination, i.e., different activation thresholds for individual *Cre*-dependent reporters, even within a same embryo, in genetically identical cell types (Figure 5D).

Issues regarding transcriptional and posttranscriptional regulation of *Cre* transcripts could introduce other biases in the experimental outcome (Sambasivan et al., 2013; Tajbakhsh, 2009; and references therein). This point is particularly important

(B) *Cre* expression in E13.5 *Myf5*^{Cre}*-DTA* embryos is restricted to a few cells whereas *Myf5* transcripts are more abundant (black arrowheads). *Myod* probe reveals severe reduction of muscles and muscle loss in the forelimb (higher power views in Figure S4D).
(C) Immunostainings of trunk sections of *Myf5*$^{CreCAP/+}$ and *Myf5*$^{CreCAP/+}$*:R26*$^{DTA/+}$ E11.5 (n = 2), E12.5 (n = 7), and E13.5 (n = 2) embryos with anti-Myf5 (red) and anti-Cre (green) antibodies. Note that while Myf5 and Cre staining colocalize extensively in control embryos at E11.5 and E12.5 (white arrowheads), Myf5^{+} cells persist in the absence of Cre expression above background levels in *Myf5*^{Cre}*-DTA* embryos.
Scale bars in (A) and (B) represent 200 μm and (C) represents 20 μm. See also Figure S4.

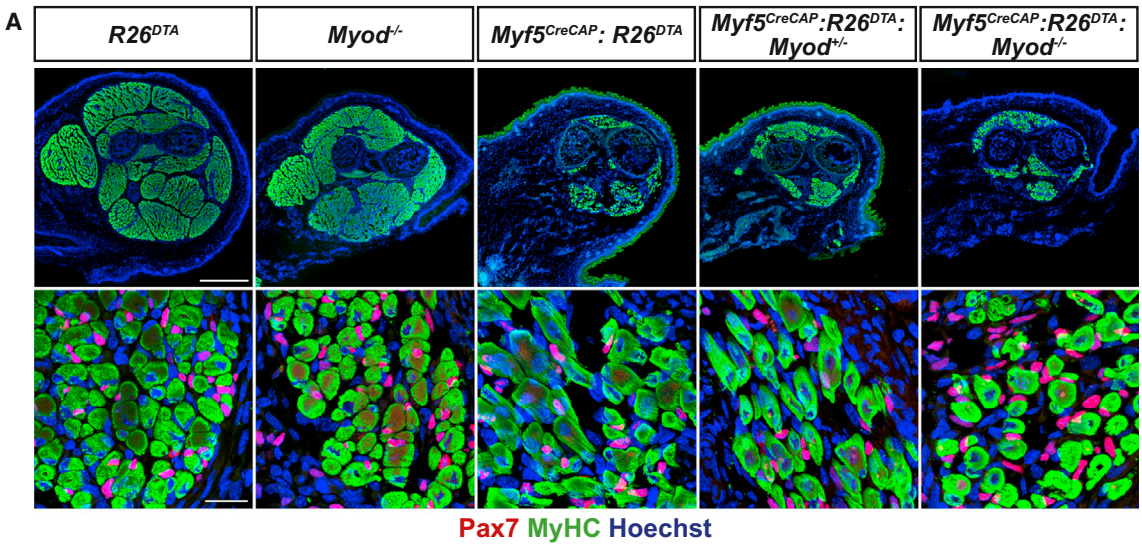

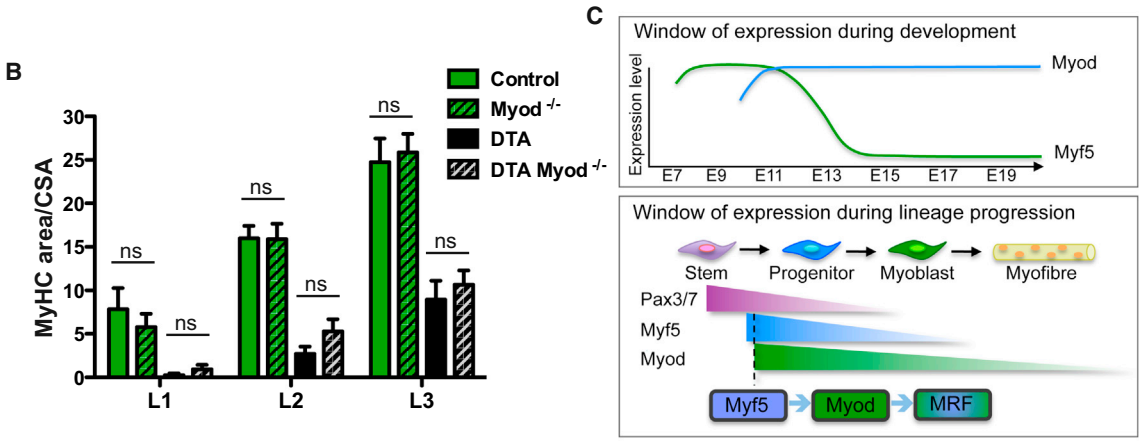

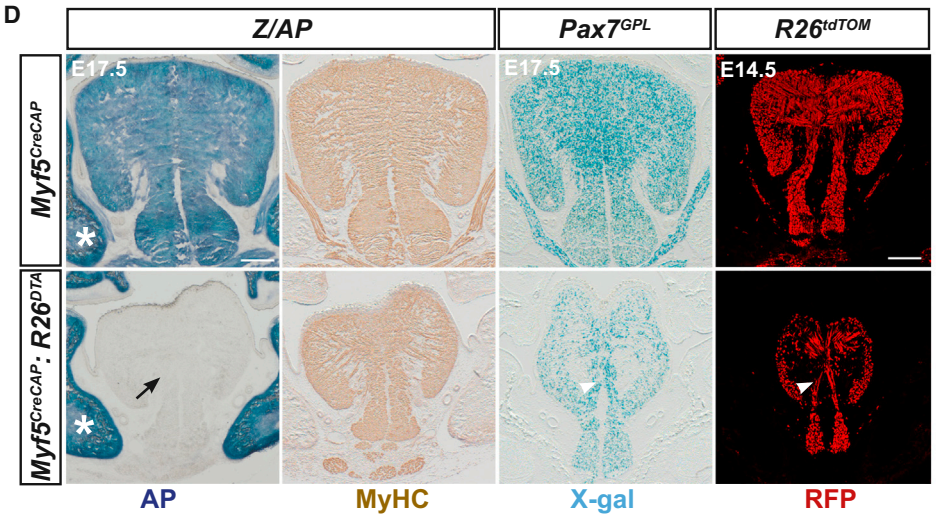

Figure 5. Muscles Persist in *Myf5*^{Cre}-*DTA* Embryos in the Absence of *Myod* Function

(A and B) Comparison of forelimb muscle ablation between E18.5 controls (*R26*$^{DTA/+}$; n = 3), *Myod*$^{-/-}$ (n = 3), *Myf5*$^{CreCAP/+}$:*R26*$^{DTA/+}$ (n = 3) and *Myf5*$^{CreCAP/+}$::*R26*$^{DTA/+}$::*Myod*$^{-/-}$ (n = 4) fetuses.

(A) Representative images of anti-MyHC (green) and anti-Pax7 (red) immunostainings of E18.5 transverse forelimb cryosections.

(legend continued on next page)

with *Myf5* where its regulation, and that of the adjacent *Mrf4* gene, is complicated by the presence of multiple unique and redundant modules extending over 100 kbp (reviewed in Carvajal and Rigby, 2010). Problems related to *Cre* misexpression have been reported previously for other tissues (e.g., Christoffels et al., 2009; Lee et al., 2013), and this is also likely to be a major factor leading to the misinterpretation of the genetic ablation data in the study by Haldar and colleagues. WM-ISH and protein immunostainings performed to compare *Cre* and *Myf5* expression gave the striking observation that *Cre* expression from the $Myf5^{CreCAP}$ allele is lost/extremely reduced in $Myf5^{Cre}$*-DTA* embryos at different developmental stages. The fact that *Myf5* transcript and protein expression persist in $Myf5^{CreCAP}$*-DTA* embryos is an indicator of the differential regulation/processing of the genetically modified (*IRES*)*-Cre* allele versus endogenous *Myf5* transcripts in vivo. In addition, a recent report (Wood et al., 2013) demonstrates a substantial reduction in the apparent level of *Myf5* expression after ablation of differentiated muscle using $ACTA1^{Cre}$. Therefore, the maintenance of *Myf5* expression appears to depend on the muscle environment, as has been shown for *Pax7* (Kassar-Duchossoy et al., 2005). Hence, in this context, *Cre* expression would be also compromised in $Myf5^{Cre}$*-DTA* embryos, further confounding its ability to perform complete ablation as required by the experimental paradigm.

In addition to these limitations, the fact that *Myf5* is expressed briefly during lineage progression and its expression levels drop drastically from mid-embryonic development (Figure 5C) make this an inappropriate gene to address lineage issues of this type unless extensive analyses using reporter gene readouts are performed concomitantly. We therefore propose that DTA-mediated kill occurs early in development, most likely within the initial peak of *Myf5*-expression, which results in complete ablation of subsets of muscles. After this time, expression of *Cre* (and thus *DTA)* is not sufficient to allow 100% elimination of $Myf5^{+}$ progenitors. Consequently, this results in cells that are (1) reporter-recombined but not ablated, or (2) neither ablated nor reporter-recombined; the latter standing as the presumed "$Myod^{+}$/*Myf5*-independent lineage." We speculate that the second wave of embryogenesis in the trunk, correlating to progenitor cells arising from the central dermomyotome in somites, is less efficiently ablated likely due to the more rapid differentiation kinetics and downregulation of *Myf5* following the onset of *Myod* expression (Tajbakhsh and Buckingham, 2000). Furthermore, differentiated muscle fibers were found to be reporter-positive in $Myf5^{Cre}$*-DTA* fetuses, hence derived from *Myf5*-expressing nonablated progenitors. Given that *Myf5* is not expressed after differentiation, these muscles will no longer be eliminated by the DTA. Therefore, because only a brief window of opportunity (Tajbakhsh and Buckingham, 2000) is available during lineage progression for Cre to recombine loxP sites from the generic *Rosa* locus (Figure 5C), it is not surprising that a $Myf5^{Cre}$*-DTA* ablation strategy gives misleading results. This is not the case for *Myod* where expression of this gene persists during lineage progression, even after permanent cell cycle exit and differentiation. Consistent with this, a recent report showed that ablation of *Myod*-expressing cells results in loss of myofibers and myogenic progenitors (defined by *Pax7* and *Myf5* expression) by E12.5 (Wood et al., 2013).

In summary, the extensive genetic data that we now provide are in discordance with the notion of a functionally significant $Myod^{+}$/*Myf5*-independent lineage. Determining whether rescue of myogenesis in these embryos is driven exclusively by expansion of nonkilled *Myf5*-derived myoblasts or also by more upstream Mrf- $Pax7^{+}$ progenitors (as proposed by Wood et al., 2013) will provide important insights into mechanisms set to regulate muscle homeostasis during development. As such, our observations alter the current view on how tissuegenesis is coordinated between cell fate genes and progenitor cell populations during skeletal myogenesis. These findings could influence the interpretation of other studies in which genetic cell ablation and lineage strategies are used to assess fundamental questions in developmental and adult stem cell biology.

EXPERIMENTAL PROCEDURES

Animal Models

Animals were handled as per European Community guidelines and protocols were approved by the ethics committee of the Institut Pasteur (CTEA). Cre recombinase, reporter, and ablator mouse lines were described previously: $Myf5^{nlacZ}$ (Tajbakhsh et al., 1996b), $Myf5^{CreCAP}$ (Haldar et al., 2008), $Myf5^{CreSOR}$ (Tallquist et al., 2000), $Myod^{m1}$ (Rudnicki et al., 1992), $Pax7^{GPL}$ (Sambasivan et al., 2013), $R26^{eGFP\text{-}DTA}$ (Ivanova et al., 2005), $R26^{lacZ\text{-}DTA}$ (Brockschnieder et al., 2004), $R26^{tdTomato}$ (*Ai9*; Madisen et al., 2010), $R26^{mTmG}$ (Muzumdar et al., 2007), $R26R^{lacZ}$ (Soriano, 1999), *Z/AP* (Lobe et al., 1999), and $Mrf4^{nlacZ}$ (Kassar-Duchossoy et al, 2004). Mice were crossed and maintained on a F1 C57/BL6:DBA2 background and genotyped by PCR. Details on mouse crosses are provided in the Supplemental Experimental Procedures.

EdU Administration In Vivo

For proliferation experiments in vivo, 5-ethyl-2′-deoxyuridine (EdU; Invitrogen E10187) was injected intraperitoneally to pregnant females at 30 μg/g body weight (6 mg/ml solution in 0.9% saline) twice at 5 and 2 hr before they were killed. EdU was detected using the Click-iT EdU Cell Proliferation Assay Kit (Life Technologies C10350) as per manufacturer's instructions.

Antibodies

Antibodies include myosin heavy chain (MyHC; rabbit polyclonal, kindly provided by G. Cossu, 1/1,000; mouse monoclonal, DSHB, 1/30), alkaline phosphatase-conjugated anti-MyHC antibody (mouse monoclonal, MY32 clone; A4335, Sigma, 1/200), Desmin (mouse monoclonal, DAKO M0760, 1/200), Myod (mouse monoclonal, 5.8.A, Dako, M3512, 1/150), Myf5 (rabbit polyclonal, Santa Cruz SC-302, 1/250), Myogenin (polyclonal, Santa Cruz sc-576, 1/100), GFP (chicken polyclonal, Abcam ab13970, 1/1,500), Pax7 (mouse monoclonal, DSHB, 1/20), Cre (mouse monoclonal, Abcam ab24607, 1/1,000),

(B) Quantification of the total myogenic zone ($MyHC^{+}$ staining/cross-sectional area, mean ± SEM) at three different forelimb levels (L1, L2, and L3). No significant (ns) differences were observed between $Myf5^{CreCAP/+}$:$R26^{DTA/+}$ and $Myf5^{CreCAP/+}$:$R26^{DTA/+}$:$Myod^{-/-}$ or $Myod^{-/-}$ and control ($Myf5^{CreCAP/+}$ or $R26^{DTA/+}$) fetuses.
(C) Schemes indicating the limited expression window available for *Myf5* globally during development and during lineage progression.
(D) Comparison of the sensitivities of *Z/AP*, $Pax7^{GPL}$, and $R26^{tdTOM}$ reporter lines in a control ($Myf5^{CreCAP/+}$, upper) and cell ablation background ($Myf5^{CreCAP/+}$:$R26^{DTA/+}$, lower) (n = 2–5 embryos/genotype). Transverse sections at the level of the tongue are shown. Note that while nonablated *Myf5*-derived cells persist according to the $Pax7^{GPL}$ and $R26^{tdTOM}$ reporters (arrowheads), this is not revealed by using the *Z/AP* transgenic reporter mouse in $Myf5^{CreCAP/+}$:$R26^{DTA/+}$ fetuses (black arrow). A section adjacent to the one stained for AP from the *Z/AP* transgene was immunostained for MyHC to identify tongue muscles. Asterisks point to endogenous AP activity from bones.
Scale bars in (A) represent low power 500 μm, high power 25 μm and (D) represents 250 μm. See also Figure S5.

and β-galactoside (rabbit polyclonal, MP Biomedicals 08559761, 1/1,500; chicken polyclonal, Immune Systems, CGAL-45A-Z, 1/1,000). tdTomato was detected with Living Colors DsRed antibody (rabbit polyclonal, Clontech 632496, 1/100).

Immunofluorescence

Immunostaining on tissue sections was performed as described elsewhere (Sambasivan et al., 2013) with modifications (see Supplemental Experimental Procedures). Images were acquired with the following systems: a Zeiss Axioplan equipped with an Apotome and ZEN software (Carl Zeiss), a Leica SPE confocal and Leica Application Suite (LAS) software or a LSM 700 laser-scanning confocal microscope and ZEN software (Carl Zeiss). All images were assembled in Adobe Photoshop and InDesign (Adobe Systems). Some images were assembled as maximum projections derived from stacks of optical sections using ImageJ (NIH). Immunostaining on whole-mount eyeballs and limbs was performed as described elsewhere (Grégoire and Kmita, 2008; Jory et al., 2009) with modifications (see Supplemental Experimental Procedures).

In Situ Hybridization and X-Gal Staining

X-gal staining and whole-mount in situ hybridization with digoxigenin-labeled antisense mRNA probes were performed as described previously (Tajbakhsh et al., 1997) and in the Supplemental Experimental Procedures.

Statistics

All experiments were carried out on a minimum of three embryos except where stated otherwise. The graphs were plotted and statistical analyses were performed using Graph Pad Prism and Microsoft Excel software. All data points are presented as mean ± SEM (error bars). The Student's t test (two-tailed, unpaired) was applied in all cases (*$p < 0.05$; **$p < 0.01$; ***$p < 0.001$) except in Figure S1G where p values were calculated by Mann-Whitney analysis. Assessment of the $MyHC^{+}$ muscle area/limb cross-sectional area was performed with Fiji (NIH) software as described in the Supplemental Experimental Procedures.

SUPPLEMENTAL INFORMATION

Supplemental Information includes Supplemental Experimental Procedures and five figures and can be found with this article online at http://dx.doi.org/10.1016/j.devcel.2014.11.005.

AUTHOR CONTRIBUTIONS

G.C., R.S., and S.T. conceived and designed the experiments and wrote the manuscript. G.C. performed most of the experiments; S.G. performed and quantitated immunostainings; and R.S. generated *Pax7*^{GPL} mice, initiated the study, and performed some of the whole-mount analysis. All authors interpreted the results, read, and approved the final manuscript.

ACKNOWLEDGMENTS

We thank M. Capecchi and P. Soriano for kindly providing *Myf5*^{Cre} mice, P. Topilko, and G. Eberl for reporter mice, and members of the lab for critical comments. We acknowledge support from the Institut Pasteur, Centre National de la Recherche Scientifique, Association Française contre les Myopathies, and the Fondation pour la Recherche Médicale.

Received: September 6, 2013
Revised: June 16, 2014
Accepted: November 4, 2014
Published: December 8, 2014

REFERENCES

Asakura, A., Hirai, H., Kablar, B., Morita, S., Ishibashi, J., Piras, B.A., Christ, A.J., Verma, M., Vineretsky, K.A., and Rudnicki, M.A. (2007). Increased survival of muscle stem cells lacking the MyoD gene after transplantation into regenerating skeletal muscle. Proc. Natl. Acad. Sci. USA *104*, 16552–16557.

Atchley, W.R., Fitch, W.M., and Bronner-Fraser, M. (1994). Molecular evolution of the MyoD family of transcription factors. Proc. Natl. Acad. Sci. USA *91*, 11522–11526.

Blitz, E., Viukov, S., Sharir, A., Shwartz, Y., Galloway, J.L., Pryce, B.A., Johnson, R.L., Tabin, C.J., Schweitzer, R., and Zelzer, E. (2009). Bone ridge patterning during musculoskeletal assembly is mediated through SCX regulation of Bmp4 at the tendon-skeleton junction. Dev. Cell *17*, 861–873.

Braun, T., and Arnold, H.-H. (1996). *Myf-5* and *myoD* genes are activated in distinct mesenchymal stem cells and determine different skeletal muscle cell lineages. EMBO J. *15*, 310–318.

Braun, T., Rudnicki, M.A., Arnold, H.H., and Jaenisch, R. (1992). Targeted inactivation of the muscle regulatory gene Myf-5 results in abnormal rib development and perinatal death. Cell *71*, 369–382.

Brockschnieder, D., Lappe-Siefke, C., Goebbels, S., Boesl, M.R., Nave, K.A., and Riethmacher, D. (2004). Cell depletion due to diphtheria toxin fragment A after Cre-mediated recombination. Mol. Cell. Biol. *24*, 7636–7642.

Carvajal, J.J., and Rigby, P.W. (2010). Regulation of gene expression in vertebrate skeletal muscle. Exp. Cell Res. *316*, 3014–3018.

Christoffels, V.M., Grieskamp, T., Norden, J., Mommersteeg, M.T., Rudat, C., and Kispert, A. (2009). Tbx18 and the fate of epicardial progenitors. Nature *458*, E8–E9, discussion E9–E10.

Cossu, G., Kelly, R., Tajbakhsh, S., Di Donna, S., Vivarelli, E., and Buckingham, M. (1996). Activation of different myogenic pathways: myf-5 is induced by the neural tube and MyoD by the dorsal ectoderm in mouse paraxial mesoderm. Development *122*, 429–437.

Frank, E., and Sanes, J.R. (1991). Lineage of neurons and glia in chick dorsal root ganglia: analysis in vivo with a recombinant retrovirus. Development *111*, 895–908.

Gayraud-Morel, B., Chrétien, F., Jory, A., Sambasivan, R., Negroni, E., Flamant, P., Soubigou, G., Coppée, J.Y., Di Santo, J., Cumano, A., et al. (2012). Myf5 haploinsufficiency reveals distinct cell fate potentials for adult skeletal muscle stem cells. J. Cell Sci. *125*, 1738–1749.

Gensch, N., Borchardt, T., Schneider, A., Riethmacher, D., and Braun, T. (2008). Different autonomous myogenic cell populations revealed by ablation of Myf5-expressing cells during mouse embryogenesis. Development *135*, 1597–1604.

Goldhamer, D.J., Brunk, B.P., Faerman, A., King, A., Shani, M., and Emerson, C.P., Jr. (1995). Embryonic activation of the myoD gene is regulated by a highly conserved distal control element. Development *121*, 637–649.

Grégoire, D., and Kmita, M. (2008). Recombination between inverted loxP sites is cytotoxic for proliferating cells and provides a simple tool for conditional cell ablation. Proc. Natl. Acad. Sci. USA *105*, 14492–14496.

Günther, S., Kim, J., Kostin, S., Lepper, C., Fan, C.M., and Braun, T. (2013). Myf5-positive satellite cells contribute to Pax7-dependent long-term maintenance of adult muscle stem cells. Cell Stem Cell *13*, 590–601.

Haldar, M., Hancock, J.D., Coffin, C.M., Lessnick, S.L., and Capecchi, M.R. (2007). A conditional mouse model of synovial sarcoma: insights into a myogenic origin. Cancer Cell *11*, 375–388.

Haldar, M., Karan, G., Tvrdik, P., and Capecchi, M.R. (2008). Two cell lineages, myf5 and myf5-independent, participate in mouse skeletal myogenesis. Dev. Cell *14*, 437–445.

Harel, I., Nathan, E., Tirosh-Finkel, L., Zigdon, H., Guimarães-Camboa, N., Evans, S.M., and Tzahor, E. (2009). Distinct origins and genetic programs of head muscle satellite cells. Dev. Cell *16*, 822–832.

Ivanova, A., Signore, M., Caro, N., Greene, N.D., Copp, A.J., and Martinez-Barbera, J.P. (2005). In vivo genetic ablation by Cre-mediated expression of diphtheria toxin fragment A. Genesis *43*, 129–135.

Jory, A., Le Roux, I., Gayraud-Morel, B., Rocheteau, P., Cohen-Tannoudji, M., Cumano, A., and Tajbakhsh, S. (2009). Numb promotes an increase in skeletal muscle progenitor cells in the embryonic somite. Stem Cells *27*, 2769–2780.

Kablar, B., Krastel, K., Ying, C., Asakura, A., Tapscott, S.J., and Rudnicki, M.A. (1997). MyoD and Myf-5 differentially regulate the development of limb versus trunk skeletal muscle. Development *124*, 4729–4738.

Kanisicak, O., Mendez, J.J., Yamamoto, S., Yamamoto, M., and Goldhamer, D.J. (2009). Progenitors of skeletal muscle satellite cells express the muscle determination gene, MyoD. Dev. Biol. *332*, 131–141.

Kassar-Duchossoy, L., Gayraud-Morel, B., Gomès, D., Rocancourt, D., Buckingham, M., Shinin, V., and Tajbakhsh, S. (2004). Mrf4 determines skeletal muscle identity in Myf5:Myod double-mutant mice. Nature *431*, 466–471.

Kassar-Duchossoy, L., Giacone, E., Gayraud-Morel, B., Jory, A., Gomès, D., and Tajbakhsh, S. (2005). Pax3/Pax7 mark a novel population of primitive myogenic cells during development. Genes Dev. *19*, 1426–1431.

Kelly, R.G. (2013). Craniofacial Muscle Development. In Stem Cells in Craniofacial Development and Regeneration, G.T.J. Huang and I. Thesleff, eds. (Hoboken: John Wiley & Sons).

Kuang, S., Kuroda, K., Le Grand, F., and Rudnicki, M.A. (2007). Asymmetric self-renewal and commitment of satellite stem cells in muscle. Cell *129*, 999–1010.

Lee, K.Y., Russell, S.J., Ussar, S., Boucher, J., Vernochet, C., Mori, M.A., Smyth, G., Rourk, M., Cederquist, C., Rosen, E.D., et al. (2013). Lessons on conditional gene targeting in mouse adipose tissue. Diabetes *62*, 864–874.

Lewandoski, M. (2001). Conditional control of gene expression in the mouse. Nat. Rev. Genet. *2*, 743–755.

Liu, J., Willet, S.G., Bankaitis, E.D., Xu, Y., Wright, C.V., and Gu, G. (2013). Non-parallel recombination limits Cre-LoxP-based reporters as precise indicators of conditional genetic manipulation. Genesis *51*, 436–442.

Lobe, C.G., Koop, K.E., Kreppner, W., Lomeli, H., Gertsenstein, M., and Nagy, A. (1999). Z/AP, a double reporter for cre-mediated recombination. Dev Biol. *208*, 281–292.

Long, M.A., and Rossi, F.M. (2009). Silencing inhibits Cre-mediated recombination of the Z/AP and Z/EG reporters in adult cells. PLoS ONE *4*, e5435.

Ma, Q., Fode, C., Guillemot, F., and Anderson, D.J. (1999). Neurogenin1 and neurogenin2 control two distinct waves of neurogenesis in developing dorsal root ganglia. Genes Dev. *13*, 1717–1728.

Ma, Q., Zhou, B., and Pu, W.T. (2008). Reassessment of Isl1 and Nkx2-5 cardiac fate maps using a Gata4-based reporter of Cre activity. Dev. Biol. *323*, 98–104.

Macharia, R., Otto, A., Valasek, P., and Patel, K. (2010). Neuromuscular junction morphology, fiber-type proportions, and satellite cell proliferation rates are altered in MyoD(-/-) mice. Muscle Nerve *42*, 38–52.

Madisen, L., Zwingman, T.A., Sunkin, S.M., Oh, S.W., Zariwala, H.A., Gu, H., Ng, L.L., Palmiter, R.D., Hawrylycz, M.J., Jones, A.R., et al. (2010). A robust and high-throughput Cre reporting and characterization system for the whole mouse brain. Nat. Neurosci. *13*, 133–140.

Murphy, M., and Kardon, G. (2011). Origin of vertebrate limb muscle: the role of progenitor and myoblast populations. Curr. Top. Dev. Biol. *96*, 1–32.

Muzumdar, M.D., Tasic, B., Miyamichi, K., Li, L., and Luo, L. (2007). A global double-fluorescent Cre reporter mouse. Genesis *45*, 593–605.

Nagy, A. (2000). Cre recombinase: the universal reagent for genome tailoring. Genesis *26*, 99–109.

Nowlan, N.C., Bourdon, C., Dumas, G., Tajbakhsh, S., Prendergast, P.J., and Murphy, P. (2010). Developing bones are differentially affected by compromised skeletal muscle formation. Bone *46*, 1275–1285.

Ott, M.-O., Bober, E., Lyons, G., Arnold, H., and Buckingham, M. (1991). Early expression of the myogenic regulatory gene, *myf-5*, in precursor cells of skeletal muscle in the mouse embryo. Development *111*, 1097–1107.

Relaix, F., and Zammit, P.S. (2012). Satellite cells are essential for skeletal muscle regeneration: the cell on the edge returns centre stage. Development *139*, 2845–2856.

Rocheteau, P., Gayraud-Morel, B., Siegl-Cachedenier, I., Blasco, M.A., and Tajbakhsh, S. (2012). A subpopulation of adult skeletal muscle stem cells retains all template DNA strands after cell division. Cell *148*, 112–125.

Rot, I., and Kablar, B. (2013). Role of skeletal muscle in palate development. Histol. Histopathol. *28*, 1–13.

Rot-Nikcevic, I., Reddy, T., Downing, K.J., Belliveau, A.C., Hallgrímsson, B., Hall, B.K., and Kablar, B. (2006). Myf5-/- :MyoD-/- amyogenic fetuses reveal the importance of early contraction and static loading by striated muscle in mouse skeletogenesis. Dev. Genes Evol. *216*, 1–9.

Rudnicki, M.A., Braun, T., Hinuma, S., and Jaenisch, R. (1992). Inactivation of *MyoD* in mice leads to up-regulation of the myogenic HLH gene *Myf-5* and results in apparently normal muscle development. Cell *71*, 383–390.

Sambasivan, R., Gayraud-Morel, B., Dumas, G., Cimper, C., Paisant, S., Kelly, R.G., and Tajbakhsh, S. (2009). Distinct regulatory cascades govern extraocular and pharyngeal arch muscle progenitor cell fates. Dev. Cell *16*, 810–821.

Sambasivan, R., Kuratani, S., and Tajbakhsh, S. (2011). An eye on the head: the development and evolution of craniofacial muscles. Development *138*, 2401–2415.

Sambasivan, R., Comai, G., Le Roux, I., Gomès, D., Konge, J., Dumas, G., Cimper, C., and Tajbakhsh, S. (2013). Embryonic founders of adult muscle stem cells are primed by the determination gene Mrf4. Dev. Biol. *381*, 241–255.

Sassoon, D., Lyons, G., Wright, W.E., Lin, V., Lassar, A., Weintraub, H., and Buckingham, M. (1989). Expression of two myogenic regulatory factors myogenin and MyoD1 during mouse embryogenesis. Nature *341*, 303–307.

Shi, X., and Garry, D.J. (2006). Muscle stem cells in development, regeneration, and disease. Genes Dev. *20*, 1692–1708.

Shinin, V., Gayraud-Morel, B., Gomès, D., and Tajbakhsh, S. (2006). Asymmetric division and cosegregation of template DNA strands in adult muscle satellite cells. Nat. Cell Biol. *8*, 677–687.

Soriano, P. (1999). Generalized lacZ expression with the ROSA26 Cre reporter strain. Nat. Genet. *21*, 70–71.

Tajbakhsh, S. (2009). Skeletal muscle stem cells in developmental versus regenerative myogenesis. J. Intern. Med. *266*, 372–389.

Tajbakhsh, S., and Buckingham, M. (2000). The birth of muscle progenitor cells in the mouse: spatiotemporal considerations. Curr. Top. Dev. Biol. *48*, 225–268.

Tajbakhsh, S., Bober, E., Babinet, C., Pournin, S., Arnold, H., and Buckingham, M. (1996a). Gene targeting the myf-5 locus with nlacZ reveals expression of this myogenic factor in mature skeletal muscle fibres as well as early embryonic muscle. Dev. Dyn. *206*, 291–300.

Tajbakhsh, S., Rocancourt, D., and Buckingham, M. (1996b). Muscle progenitor cells failing to respond to positional cues adopt non-myogenic fates in myf-5 null mice. Nature *384*, 266–270.

Tajbakhsh, S., Rocancourt, D., Cossu, G., and Buckingham, M. (1997). Redefining the genetic hierarchies controlling skeletal myogenesis: *Pax-3* and *Myf-5* act upstream of *MyoD*. Cell *89*, 127–138.

Tallquist, M.D., Weismann, K.E., Hellström, M., and Soriano, P. (2000). Early myotome specification regulates PDGFA expression and axial skeleton development. Development *127*, 5059–5070.

von Maltzahn, J., Jones, A.E., Parks, R.J., and Rudnicki, M.A. (2013). Pax7 is critical for the normal function of satellite cells in adult skeletal muscle. Proc. Natl. Acad. Sci. USA *110*, 16474–16479.

Vooijs, M., Jonkers, J., and Berns, A. (2001). A highly efficient ligand-regulated Cre recombinase mouse line shows that LoxP recombination is position dependent. EMBO Rep. *2*, 292–297.

Wood, W.M., Etemad, S., Yamamoto, M., and Goldhamer, D.J. (2013). MyoD-expressing progenitors are essential for skeletal myogenesis and satellite cell development. Dev. Biol. *384*, 114–127.

Wu, S., Wu, Y., and Capecchi, M.R. (2006). Motoneurons and oligodendrocytes are sequentially generated from neural stem cells but do not appear to share common lineage-restricted progenitors in vivo. Development *133*, 581–590.

Yin, H., Price, F., and Rudnicki, M.A. (2013). Satellite cells and the muscle stem cell niche. Physiol. Rev. *93*, 23–67.

Zhao, X., Yu, Q., Huang, L., and Liu, Q.X. (2014). Patterns of positive selection of the myogenic regulatory factor gene family in vertebrates. PLoS ONE *9*, e92873.